

Original article

Christian Heinrich* and Veera Sundararaghavan

A method to predict fatigue crack initiation in metals using dislocation dynamics

DOI 10.1515/corrrev-2017-0045

Received November 2, 2016; accepted June 12, 2017

Abstract: A theory is proposed to predict the initiation of fatigue cracks using cyclic dislocation dynamics (DD) simulations. The evolution of dislocation networks in a grain is simulated over several cycles. It is shown that the dislocation density and the energy stored in the dislocation networks increase with the number of cycles. The results of the DD simulations are used to construct an energy balance expression for crack initiation. A hypothetical crack is inserted into the grain, and the Gibbs energy consisting of the energy of the dislocation structure, the surface energy of the hypothetical crack, and the reduction in continuum energy is evaluated. Once the Gibbs energy attains a maximum, the dislocation structure becomes unstable, and it becomes energetically more favorable to form a real crack. The proposed method is applied to oxygen-free high conductivity copper, and the results are compared against experiments. Finally, it is shown how the method can be amended to account for environmental effects.

Keywords: crack; dislocation dynamics simulation; fatigue.

1 Introduction

Persistent slip bands (PSBs) are recognized as a precursor to fatigue crack initiation, especially in ductile FCC materials (Forsyth, 1953; Mughrabi & Wang, 1982; Sangid et al., 2011; Sangid, 2013). PSBs and other dislocation arrangements from cyclic loading are mostly found in copper and copper alloys (Lukáš et al., 1968; Winter, 1974; Mughrabi, 1978). But they can also be observed in fatigued magnesium (Stevenson & Vander Sande, 1974; Kwadjo &

Brown, 1978), ferrite steel (Yumen & Huijiu, 1986), aluminum (Forsyth, 1953), and titanium (Zhang et al., 1998). At lower plastic strains, channel or ladder features can be observed, running through the matrix structure (Finney & Laird, 1975; Essmann & Mughrabi, 1979). This unique dislocation structure is formed in an attempt to minimize the energy of the system (Basinski & Basinski, 1992).

Together with the early experimental studies of fatigue behavior of metals emerged analytical and qualitative theories regarding dislocation arrangements and their role in fatigue crack initiation (Mott, 1958; Antonopoulos et al., 1976; Essmann et al., 1981). However, numerical investigations of dislocation structures took place much later. The first study to numerically investigate the evolution of dislocation structures using dislocation dynamics (DD) simulation was performed by Amodeo and Ghoniem (1990). They showed how dislocations can assemble into organized structures such as PSBs and dislocation cells. In their study, PSBs arose from enhanced dislocation multiplication and formed stable dipole structures.

So far, dislocations as the main driver for plastic deformation in metals have not been investigated thoroughly in the context of fatigue crack *initiation*. Numerical studies on the topic are usually restricted to crystal plasticity finite element (CPFE) simulations (Fine & Bhat, 2007; Joseph et al., 2010; Li et al., 2015), while theories that incorporate dislocations are mostly analytic (Mura & Nakasone, 1990) in nature or consider two-dimensional (2D) arrangements (Deshpande et al., 2003; Huang et al., 2014). There have also been some attempts to incorporate three-dimensional (3D) effects into 2D DD simulations (Benzerga et al., 2004; Brinckmann, 2005).

It has been pointed out that it is important to incorporate the true 3D nature of dislocation motion in order to fully understand the evolution of dislocation networks (Déprés et al., 2014). Some of the truly 3D DD simulations to investigate fatigue behavior were done by Déprés and co-workers. Déprés et al. (2004) performed discrete DD simulations of AISI316L steel surface grains. They proposed a mechanism of the emergence of slip bands, which were observable in DD simulations after only a few cycles. In their calculations, dislocation loops emerge from a

*Corresponding author: Christian Heinrich, Department of Aerospace Engineering, University of Michigan, 1320 Beal Ave., Ann Arbor, MI 48109-2140, USA, e-mail: cheinric@umich.edu

Veera Sundararaghavan: Department of Aerospace Engineering, University of Michigan, 1320 Beal Ave., Ann Arbor, MI 48109-2140, USA

single Frank-Read source and eventually pile up against the grain boundary. At some time, pile-up saturation is reached and cross-slip occurs in appreciable amounts, producing Koehler-type dislocation sources that also emit dislocations in their respective plane. The slip bands thicken and eventually rearrange in stable dipole structures. Based on this background, further studies were done by Shin et al. (2007) where the influence of precipitates on the early fatigue behavior was investigated. Déprés et al. were able to numerically reproduce dislocation structures observed in fatigue experiments. However, a theoretical treatment of when these dislocation structures form a crack surface is not well understood. In a series of papers, Mura and co-workers (Tanaka & Mura, 1981; Mura & Nakasone, 1990; Venkataraman et al., 1991; Mura, 1994) developed and refined a theory for the initiation of fatigue cracks in metals. In the theory, dislocations accumulate in a slip band as cycling progresses. The Gibbs free energy is tracked over a number of cycles and attains a maximum at some point, which indicates the initiation of a fatigue crack. At this point, the dislocation structure in the slip band becomes unstable, and it is energetically more favorable to form a free surface, nucleate a fatigue crack, and extrude part of the slip band than increasing the dislocation density in the slip band further. The key component of this theory is the understanding of the stored energy of the dislocation structure as a function of strain and number of loading cycles. Only recently has the computational power sufficiently advanced to study the energetics of 3D dislocation structures over sufficient level of strains and number of cycles. Déprés et al. (2014) were able to capture evolution of dislocation in a 22- μm -diameter grain over a maximum of 24 cycles and maximum equivalent plastic strain amplitude of 1.5×10^{-3} . Primary contribution of this work is to advance the energy-based theory using large-scale DD simulations and develop a methodology to translate the DD results towards predictive modeling of fatigue crack initiation in solids.

2 Energy contributions for fatigue crack initiation

In the theory presented by Mura et al., the change in Gibbs free energy ΔG of the fatigue crack initiation process is given by

$$\Delta G = E_{\text{surf}} - E_{\text{cont}} - E_{\text{disl}}. \quad (1)$$

Here E_{cont} is the loss of continuum energy due to crack initiation, and the explicit mathematical form depends on

the geometry of the specimen, the loading conditions, and the crack shape. E_{disl} is the energy stored in the dislocation structure with the different contributions explained in Section 4. $E_{\text{surf}} = 2A\gamma$ is the surface energy, where A is the surface area, γ is the energy per surface area, and factor 2 reflects the fact that two surfaces are created once a crack forms. All energy contributions are evolving over the cycle number n .

A crack is nucleated once it is energetically more favorable to create a free surface instead of increasing the energy stored in the dislocation structure with continued cycling. Thus,

$$\frac{d\Delta G}{dn} = 0 \quad (2)$$

indicates crack nucleation.

The minus sign of E_{disl} in equation (1) is intentional. One would expect that the energy of the dislocation structure represents plastic deformation that requires additional energy to occur and thus hinders crack growth and increases effective surface energy or fracture toughness. Orowan (1955) extended the surface energy by a plastic work term to yield $\gamma + \gamma_p$. For plastically deforming solids, γ_p is orders of magnitudes larger than γ . However, this plastic work term is dissipative in nature and related to the damping of dislocation motion E_{damp} as explained in detail in Section 4. On the other hand, E_{disl} represents energy that is stored in the dislocation structure. When dislocations are piled up against each other, they are at an elevated energy state, which could be lowered by removing these dislocations. Therefore, E_{disl} represents energy that is available to nucleate a crack. It has the same sign as the loss in strain energy of the continuum, which, in the classical theory of crack propagation, is the driver for crack advancement. The loss of strain energy density due to crack nucleation as well as loss of elastic energy of the dislocation networks balances out the energy of the newly created crack surfaces.

Equation (1) can be compared with the classical Griffith criterion for crack advancement. In the case of an infinite plate of unit thickness, with far field stress σ , crack size $2a$, and Young's modulus E , the surface energy is $E_{\text{surf}} = 4a\gamma$ and the decrease in strain energy is

$$E_{\text{cont}} = -\frac{\pi a^2 \sigma^2}{E}.$$

Sustained crack growth occurs once $\frac{d(\Delta G)}{da} = 0$ (Sanford, 2002).

Mura's theory was also further developed in the context of CPFEE simulations by Fine and Bhat to predict fatigue initiation in steel (Bhat & Fine, 2001) and iron and copper (Fine & Bhat, 2007). Li et al. (2015) used their

approach to predict fatigue crack initiation in an aluminum alloy. In all these studies, an energy balance of the form

$$\Delta G = -E_{\text{cont}} - An\delta + 2A\gamma \quad (3)$$

was constructed. Variable $2A\gamma$ represents the surface energy. $-E_{\text{cont}}$ is the reduction in elastic energy stored in the specimen when a crack is formed. For a half penny-shaped crack, $E_{\text{cont}} = \frac{4(1-\nu^2)}{3E}\sigma^2 a^3$, where E is the elastic modulus, ν is Poisson's ratio, σ is the applied stress, and a is the radius of the crack. $An\delta$ represents the portion of the external work during cyclic loading, where n is the number of cycles and the parameter δ is given by (Fine & Bhat, 2007)

$$\delta = ft_m \frac{\Delta\tau \Delta\gamma_p}{2} \quad (4)$$

The term f is an energy efficiency factor, t_m is the maximum PSB width, $\Delta\tau$ is the shear stress range at a point, and $\Delta\gamma_p$ is the maximum shear strain at the same location. The efficiency factor is calibrated from CPFEE simulations and usually on the order of a few percentages. The term $An\delta$ represents energy stored in the solid that may be used at a later point to advance a crack. The majority of the external work (so the fraction of $1-f$) is dissipated as heat. The energy stored in the solid $An\delta$ is similar in nature to E_{disl} , as discussed earlier. The former captures energy stored in the solid macroscopically through crystal plasticity, while the latter explicitly sums up the energy of individual dislocation segments. In contrast to the theory by Mura et al., Fine and Bhat assumed that a small crack is already present in the solid. The crack size increases with number of cycles and reaches a critical value when $\frac{d\Delta G}{da} = 0$.

Another study that focuses on the energies associated with fatigue crack initiation was done by Sangid et al. (2011). They include continuum terms for the externally applied stress, work hardening, and dislocation pile-up. Also included are atomistic terms for dislocation nucleation, dislocation-grain boundary interaction/extrusion, and shearing of matrix and precipitates (this is specific to the super alloys investigated). Fatigue crack initiation happened when the energy of the PSB turned unstable with respect to slip in the PSB: $\frac{\partial \Delta G}{\partial X} = 0$, where X is the slip in

the PSB. To evolve the dislocation density in the model, Sangid relied on an empirical fit (*in situ* neutron diffraction measurements) from the literature (Huang et al.,

2008) of the form n^c . Compared to the theory presented so far, Sangid et al. (2011) incorporate the influence of grain boundaries and the extrusions the dislocation pile-up forms.

3 DD simulation

3.1 Method

The current study aims to expand the theory presented by Mura et al. The goal is to replace terms that were derived analytically and for an idealized 2D dislocation structure with numerical results obtained from 3D DD simulation of a more realistic dislocation structure. DD has the advantage that it captures the main mechanism of inelastic deformation in metals, namely, dislocations, which could otherwise only be achieved by molecular dynamics (MD) simulations. Compared to MD, DD simulations can span significantly larger time and length scales. Typical DD simulation sizes are on the order of several micrometers, and simulations time is on the order of microseconds.

In 3D DD simulations, the dislocations are explicitly discretized as nodes connected by line segments (Bulatov et al., 2004; Bulatov & Cai, 2006; Arsenlis et al., 2007; Zbib, 2012). The nodes move due to Peach-Koehler-Forces, which arise from externally applied loads and from interactions with other dislocation segments. A resulting velocity is derived from the forces through a mobility law. The velocities are integrated through an explicit or implicit time integration scheme, and the position of the nodes is updated. Finally, topological operations might be performed such as splitting or merging segments and insertion or removal of nodes. DD simulations were performed using the PARAllel DISlocation Simulator ParaDiS (Bulatov et al., 2004; Arsenlis et al., 2007) developed at Lawrence Livermore National Laboratory.

3.2 Assumptions

Some assumptions and approximations that might impact the results during the DD fatigue simulations should be acknowledged. The following is mostly due to the methods related to DD or the available version of ParaDiS in particular:

- In order to simulate a sufficient amount of cycles in the given computational time, the strain rates need to be set to be sufficiently high.
- The dislocation discretization is finite. Dislocation segments are between 100 b and 2000 b (≈ 25 nm–500 nm) in length.

- Zero-order grain boundaries: Grain boundaries are included. Dislocations may pile-up against the grain boundary, but no intrusion/extrusion takes place. The grain boundary simply acts as a barrier, but dislocations may move inward again, if the resulting forces are acting accordingly. The grain is assumed to be spherical.
- Single crystal elasticity solution used for DD: The resulting forces on the dislocations are based on a single crystal infinite medium. In the simulation, no dislocations are placed outside of the grain. This can be justified by considering evolution of dislocations in different grains whose long-range effects and stress fields are shielded by the grain boundary.
- No free surfaces are considered: The proposed methodology does not account for free surfaces, where dislocations can leave the medium. Until crack nucleation, no free surfaces exist. Dislocations are assumed to be pushed out or form a free surface at fatigue crack initiation, but it is not exactly specified how this happens.
- Cross-slip in ParaDiS is determined based on projected forces. If a dislocation is screw, or almost screw in character, the forces acting on the dislocation are calculated in the current glide plane, as well as the projected forces in potential cross-slip planes. If the projected forces in the potential cross-slip plane are larger than in the current glide plane, then the dislocation undergoes cross-slip. In principle, this type of cross-slip can happen very easily, as there is no further energy required for cross-slip. Also, this type of cross-slip mechanism can accommodate, for example, the glide from primary to cross and back to primary plane that is identified by Déprés et al. (2014) as a source for slip bands.

On the other hand, thermally activated cross-slip is not included as such. In thermally activated cross-slip, there is a combination of partials before cross-slip can happen or dissociation into partials and then cross-slip occurs as explained by Fleischer (1959) and Escaig (1968). These mechanisms are not present in ParaDiS in this way.

4 Energy contributions in DD simulations

During DD simulations, a variety of energy contributions need to be taken into account. As the evolution of the energy stored in the dislocation network is a major ingredient in the proposed method to predict fatigue

crack initiation, the energy terms will be explained here in detail. Generally speaking, the energy can be divided into an internal energy and an external work contribution.

$$E_{\text{tot}} = \underbrace{E_{\text{disl-disl}} + E_{\text{self}} + E_{\text{core}} + E_{\text{damp}} + E_{\text{anni}} + E_{\text{el,int,cont}}}_{\text{internal}} - \underbrace{W_{\text{ext}}}_{\text{external}}. \quad (5)$$

The total energy E_{tot} should be constant but does not need to be zero. If dislocation networks are present in the solid initially, then the initial energy, without any external loads applied, is $E_{\text{tot,ini}} = E_{\text{disl-disl}} + E_{\text{self}} + E_{\text{core}}$. These three energy contributions also make up the total energy of the dislocation structure at any given point in time as given by E_{disl} in Section 2.

The individual terms in equation (5) are as follows:

- $E_{\text{disl-disl}}$ describes elastic energy of interacting dislocations. The energy is calculated for piecewise straight dislocation segments. The energy is calculated for each segment interacting with every other segment, without double counting: $E_{\text{disl-disl}} = \sum_{i=1}^{N-1} \sum_{j=i+1}^N E_{\text{disl-disl},ij}$. $E_{\text{disl-disl},ij}$ is the energy of the elastic interaction between dislocation segment i and dislocation segment j . The elastic interaction energy is calculated using a non-singular continuum theory of dislocations as described by Cai et al. (2006). Here the Burgers vector is spread out in a non-local fashion to remove the singularity that would otherwise result when integrating the stress field around dislocations. The dislocation driving force in ParaDiS (Arsenlis et al., 2007), the computer program used for this study, is based on the same theory. The dislocation interaction force depends both on length and relative position of the various dislocations.
- E_{self} is the energy due to the self force of the dislocations. This is equivalent to $\sum_N E_{\text{disl-disl},ii}$. The energy due to self force only depends on the length of the dislocation segments.
- E_{core} is the core energy of the dislocations. These are energy contributions that cannot be accounted for by the linear elastic model that is used as the bases for DD simulations. Core energy contribution should only be short ranged in nature and extend for a few atoms (Henager Jr. & Hoagland, 2005). In this study, $E_{\text{core}} = \sum_{\text{segments}} \frac{\epsilon_{\text{core}}}{(1-\nu)} [\mathbf{b}_i \circ \mathbf{b}_i - \nu(\mathbf{b}_i \circ \mathbf{t}_i)] l_i$. Here ϵ_{core} is the core energy per unit length, ν is Poisson ratio, \mathbf{b}_i is the Burgers vector, \mathbf{t}_i is the orientation, and l_i is the length of the line element.
- E_{damp} is the damping energy. It is the energy that is dissipated when dislocations move. In an experiment,

the dissipation would be noted in the form of heat. The total energy dissipated up to a given time t is expressed by $E_{\text{damp}}(t) = \int_0^t \sum_{\text{nodes}} \mathbf{F}_i \circ \mathbf{v}_i dt$. Here \mathbf{v}_i denotes the velocity of node i of the discretized dislocation network and \mathbf{F}_i denotes the force acting on that node.

- E_{anni} is the energy lost in annihilation. In the DD simulations, topological operations (node insertion, segment merge, segment deletion, etc.) are performed after every time step. During such a topological operation, it is possible for segments that are within a sufficiently close range (a few Burgers vectors separation) and that have proper signs to annihilate. In reality this event would include motion of atoms and dissipation of energy. However, in the DD simulations, this event is purely governed by an algorithm, and therefore, the resulting loss in energy has to be accounted for separately. The annihilated energy is based on the core energy and the length of the dislocations that annihilate.
- $E_{\text{el,int,cont}}$ is the internal continuum energy. The dislocations are embedded into this continuum. $E_{\text{el,int,cont}}(t) = \int_V \int_0^{\varepsilon(t)} \sigma_{ij} d\varepsilon_{ij} dV$. Here V is the grain volume, σ_{ij} and ε_{ij} are stress and strain components, respectively. The continuum is isotropic linear elastic, and the applied stress is uniaxial, which results in the simplified expression $E_{\text{el,int,cont}}(t) = \frac{V(\sigma_{\text{ext}}(t))^2}{2E}$. $\sigma_{\text{ext}}(t)$ is the externally applied uniaxial stress at time t , and E is the elastic modulus of the material.
- W_{ext} is the work done due to externally applied load. Usually, the load would be applied in the form of traction or displacement. However, ParaDiS assumes an infinite solid. As a result, external loads are applied as a homogeneous stress field. The work performed up to a certain moment is $W_{\text{ext}}(t) = \int_V \int_0^{\varepsilon(t)} \sigma_{\text{ext}} d\varepsilon dV = \int_V \int_0^t \sigma_{\text{ext}} \dot{\varepsilon} dt dV$, where $\dot{\varepsilon}$ is the strain rate.

5 Example of energy evolution in DD simulations

An example of creep in a solid will highlight the evolution of energy contributions during DD simulations, which will form the bases for the method to determine the fatigue crack nucleation later on. Originally, the solid only contains a single Frank-Read source. External load is applied through a uniaxial step stress; the load is held for some time and eventually removed. The applied load

and the resulting increase in dislocation density are given in Figure 1.

The evolution of the dislocation structure is shown in Figure 2. Figure 2A shows the initial Frank-Read source, and Figure 2B displays a dislocation that bows out due to the externally applied stresses. The Frank-Read source subsequently continues to bow out and create dislocation loops. The dislocations pile up against the grain boundary. The space between individual dislocation loops increase when going further inward, as shown in Figure 2C. After the external load is removed, the loops collapse again and move towards their origin, as seen in Figure 2D. Subsequently, the loops annihilate, such that at the end of the simulation, only one full loop remains, which eventually would also vanish, leaving behind only the original Frank-Read source.

The evolution of the energy terms for the creep simulation of the Frank-Read source is shown in Figure 3. It is worth to point out the curves for the elastic internal energy stored in the continuum $E_{\text{el,int,cont}}$ and the external work W_{ext} . The internally stored work is constant as long as the applied stress does not change and pertains to the elastically stored energy of the perfect crystal. Any nonlinearities regarding the internally stored or dissipated energy are due to dislocation motions and accounted for separately. On the other hand, the external work is not constant and increases over time because the solid deforms under non-zero external applied stress. A major portion of the performed work is stored as elastic energy in the solid and recovered once the load is removed, as seen in Figure 3 at time $t = 3.7 \times 10^{-5}$ s. However, upon removal of the external load, not all of the external work is recovered. The remainder either went into creation of

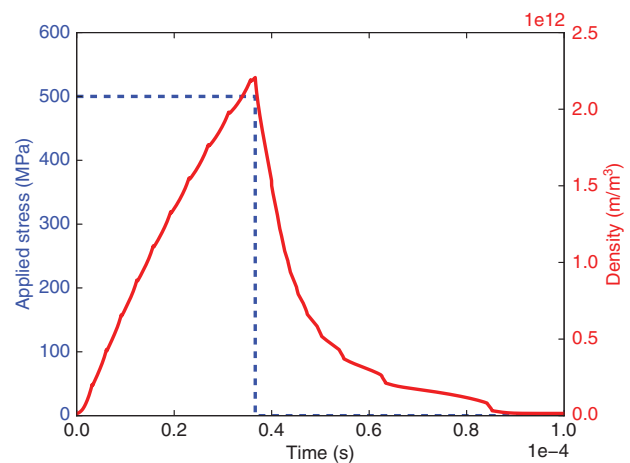


Figure 1: Applied stress (—) and resulting increase in dislocation density (—) during creep of a Frank-Read source.

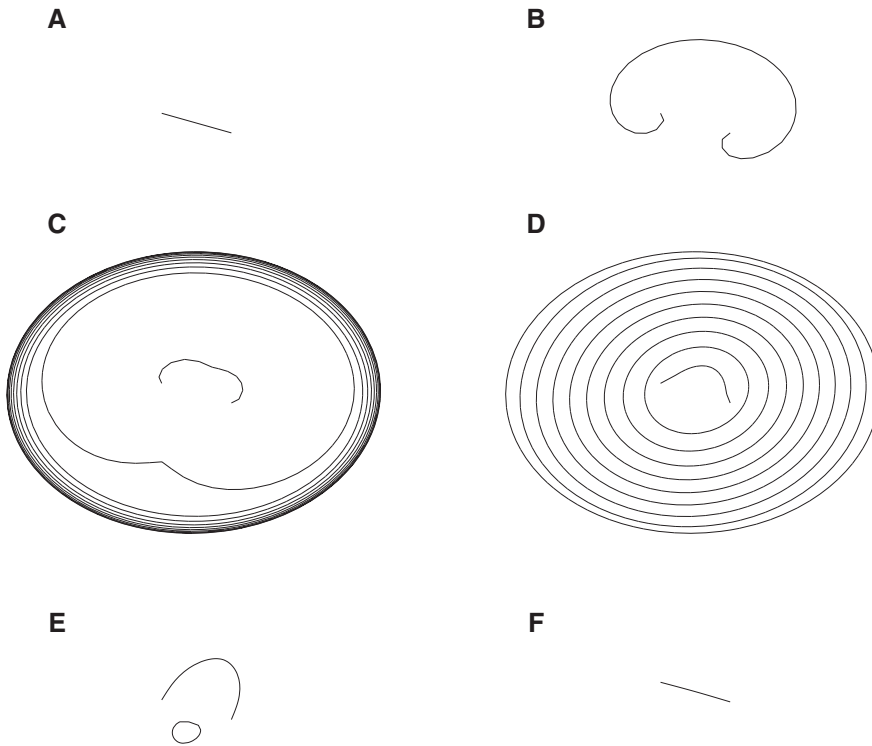


Figure 2: Frank-Read source in creep simulation. (A) Initial configuration, $t=0$ s. (B) Bowing out, $t=2.2 \times 10^{-6}$ s. (C) Maximum pileup of dislocations, $t=3.7 \times 10^{-5}$ s. (D) Collapse of dislocation loops after load removal, $t=4.1 \times 10^{-5}$ s. (E) Last collapsing loop, $t=8.5 \times 10^{-5}$ s. (F) Final simulation frame, $t=1.0 \times 10^{-4}$ s.

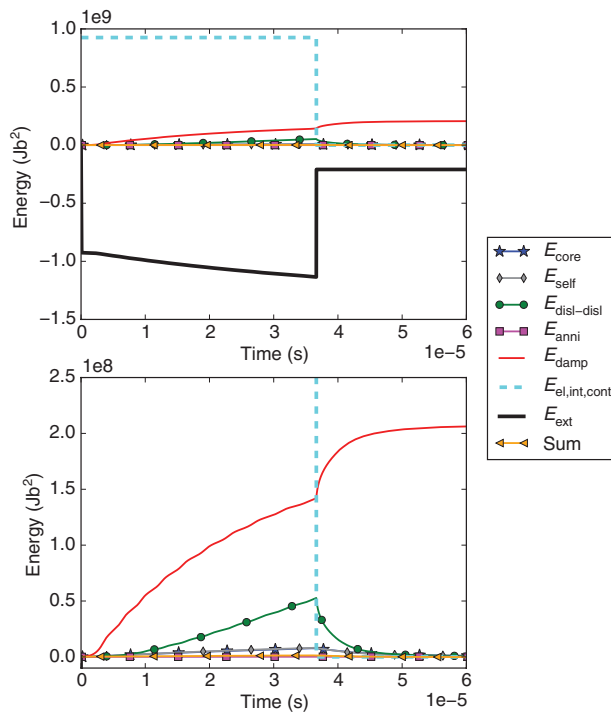


Figure 3: Evolution of energy terms in a DD simulation of a Frank-Read source in creep. Both curves show the same, with the axes-range of the bottom curve adjusted to better display energy terms of smaller magnitude.

the dislocation network and the interaction of dislocations ($E_{\text{core}} + E_{\text{self}} + E_{\text{disl-disl}}$) or into moving the dislocations and dissipation. Once the external load is removed, the remaining energy stored in the dislocation network is exchanged to reverse the motion of the dislocation movement. As a result, E_{damp} in Figure 3 increases further after $t=3.7 \times 10^{-5}$ s, while $E_{\text{core}} + E_{\text{self}} + E_{\text{disl-disl}}$ tends to be zero. This behavior is analogous to the one shown in the previous section.

6 Calculation of fatigue crack initiation

6.1 Simulation details

DD simulations were performed for pure copper, as this material has been extensively studied in the literature. While the previous example used the most basic FCC material law offered by ParaDiS, “FCC_0”, the fatigue DD simulations employ the “FCC_climb” mobility law. This mobility is an alternative to the “FCC_0”. It permits dislocations to climb a small amount and drift out of the glide

plane. The mobility automatically sets flags to allow cross-slip and enforce glide planes. However, this is not strictly enforced, allowing some flexibility in the rediscrretization step of ParaDiS, which results in an overall improvement in simulation time step size (Arsenlis et al., 2011). When comparing fatigue DD simulations using “FCC_0” versus “FCC_climb” mobilities, it was found that the latter leads to 1–2 magnitudes larger time steps. The elastic modulus and mobilities used in this study are the default values also used in the latest public ParaDiS release (Arsenlis et al., 2011) as test cases. The material properties are summarized in Table 1.

As stated previously, the loading rate is chosen very high ($1 \times 10^5/s$). This is necessary to allow for a sufficient number of cycles to be calculated. The typical size of a simulation increment is between 1×10^{-12} and 1×10^{-14} s. As the simulation advances, the step size gets progressively smaller due to an increase in dislocation density and more nodes of the discretized dislocation network being in close proximity (Gardner et al., 2015). It was also noticed that the simulation time increment significantly reduces after load reversal.

The load is applied in the x-direction with respect to the crystal frame, and a maximum strain amplitude of 0.3% is prescribed. The loading is also depicted in

Figure 4. The most important simulation parameters are summarized in Table 2.

The size of the grain is $20,000 b \approx 5 \mu\text{m}$ in diameter.

The initial microstructure is chosen to be 12 dislocation loops of random location. The loops have a side length of $3333 b$, and there is one loop for every FCC slip system. The loops are randomly clustered in the center of the simulation volume/the center of the simulated grain. The assumption here is that the initial dislocation configuration has no influence on the morphology of the microstructure after a sufficient number of cycles as pointed out by Déprés et al. (2014). Compared to Déprés et al. (2014), loops are used as a seed instead of Frank-Read sources. The initial microstructure is given in Figure 5A.

6.2 Simulation results

The evolution of the density is shown in Figure 6. There are two peaks in dislocation density per full loading cycle: one around maximum tensile strain and one around maximum compressive strain. During every cycle, the peak value in dislocation density lags behind the peak in applied strain. Even when strain levels are decreasing, there is still a significant stress applied on the solid, which exerts a force on dislocations and causes them to increase in density.

It can be noted that with increasing number of cycles, density increases. However, the speed at which this happens slows down. Different opinions can be found in the literature. Mura and Nakasone (1990) and Mura (1994) and Fine and Bhat (2007) suggested a linear increase in dislocation density with respect to cycles for a sufficiently large number of cycles, while Brinckmann (2005) showed a $\log(n)$ increase of density with number of cycles. Huang et al. (2008) found a power law dependence in Hasteloy X, which Sangid et al. (2011) fit empirically to $\rho = A_1 n^{c_1} + A_2$, where ρ is the dislocation density, n is the number of cycles, and A_1 , A_2 and c_1 are fitting constants.

Table 1: Material properties.

Description	Value	ParaDiS keyword
Mobility law	FCC climb	mobilityLaw
Shear modulus	54.6 GPa	shearModulus
Poisson's ratio	0.324	pois
Burgers vector magnitude	2.556×10^{-10} m	burgMag
Young's modulus	144.58 GPa	YoungModulus
Dislocation core radius	5 b	rc
Dislocation core energy	16.99747×10^9 J/b	Ecore
Screw dislocation mobility	$1 \times 10^4 / (\text{Pa} \cdot \text{s})$	MobScrew
Edge dislocation mobility	$1 \times 10^4 / (\text{Pa} \cdot \text{s})$	MobEdge

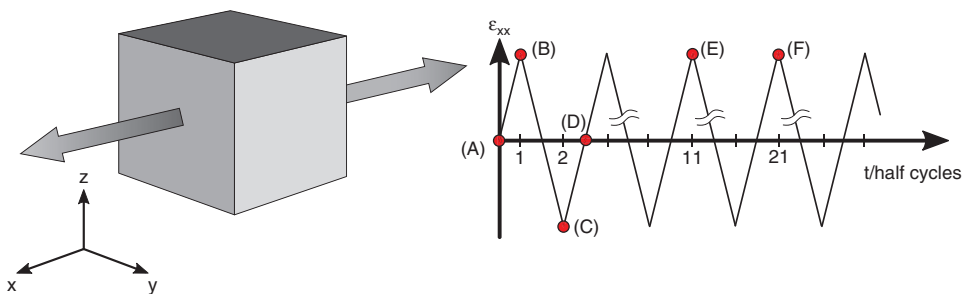


Figure 4: Uniaxial loading during fatigue DD simulations. The letters indicate subfigures in Figure 5.

Table 2: Simulation parameters.

Description	Value	ParaDiS keyword
Strain rate	$1 \times 10^5/s$	eRate
Strain amplitude	0.3%	eAmp
Loading conditions	Strain controlled cyclic loading	loadType=4
Time integration procedure	trapezoid	timestepIntegrator
Time integration tolerance	1.25	rTol
Maximum segment length	2000 b	maxSeg
Grain diameter	20,000 b	n.A.

A plot of plastic strain at peak load during each cycle is given in Figure 7. The plastic strain increases from about 0.07% in the first cycle to 0.095% in the 10th cycle and decreases to around 0.9% in further cycles.

Similarly, applied stress in the loading direction as a function of cycle number is depicted in Figure 8. Slight softening can be observed during the initial cycles, but the stress levels eventually stabilize around 300 MPa.

Finally, stress as a function of strain during the 1st, 5th, and 15th cycles is plotted in Figure 9. The hysteresis loops are stable, but a small softening can be seen between cycle 1 and later cycles.

A direct comparison of the presented data with experimental results is not readily possible due to the small grain size and high loading rates used in the DD simulations. It can be noted that the stress given in Figures 8 and 9 is higher than expected from oxygen-free high conductivity (OFHC) copper. However, many monotonic and fatigue tests use annealed copper, which have grain sizes of tens to hundreds of micrometers (Kim & Laird, 1978;

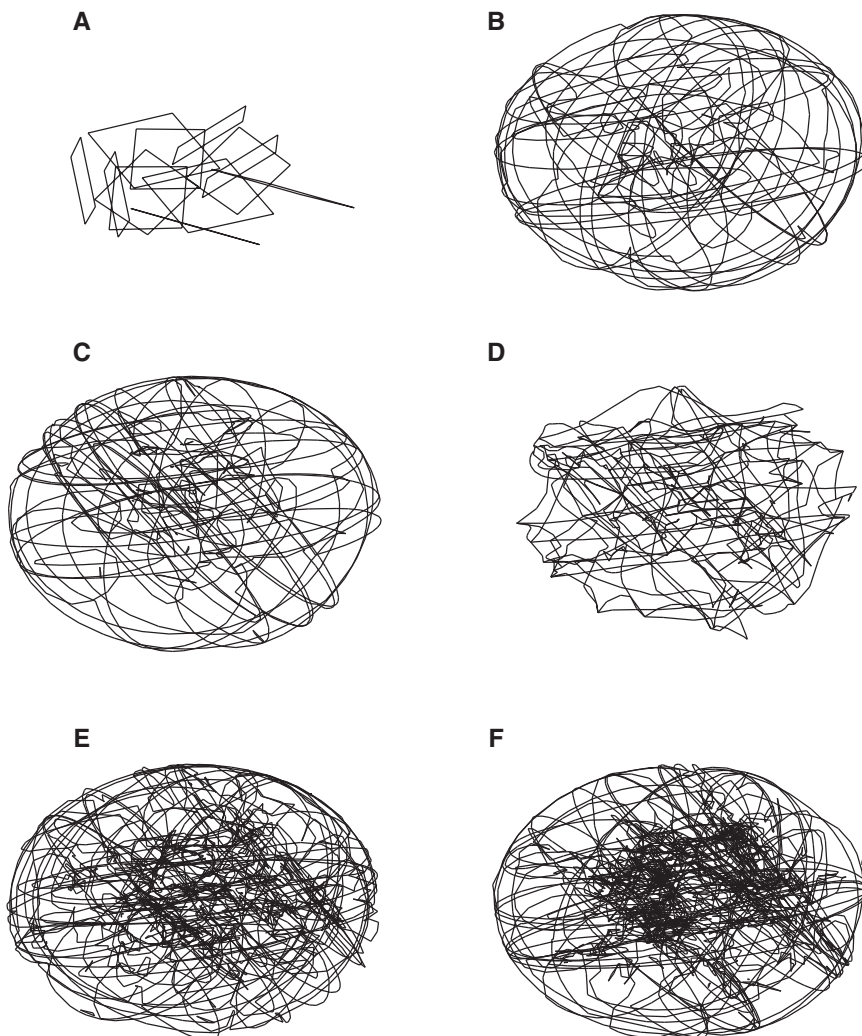


Figure 5: Evolution of dislocation networks. (A) $t=0.0$ s, initial configuration. (B) $t=3.02 \times 10^{-8}$ s, maximum tensile strain after initial loading during first cycle. (C) $t=9.01 \times 10^{-8}$ s, maximum compression strain in first full cycle. (D) $t=1.20 \times 10^{-7}$ s, zero applied strain, after first cycle. (E) $t=6.30 \times 10^{-7}$ s, maximum tensile strain after 5 full cycles/11 half cycles. (F) $t=1.23 \times 10^{-6}$ s, after 10 full cycles/21 half cycles.

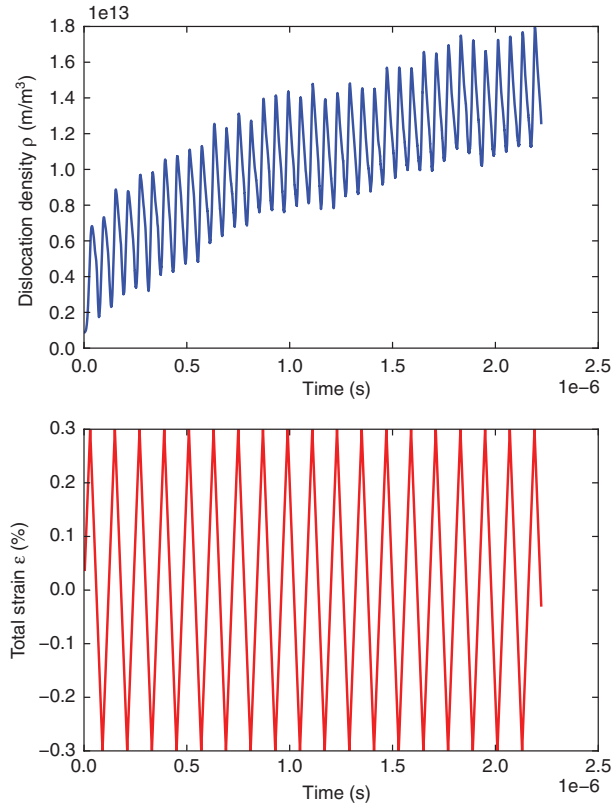


Figure 6: Dislocation density evolution and applied strain.

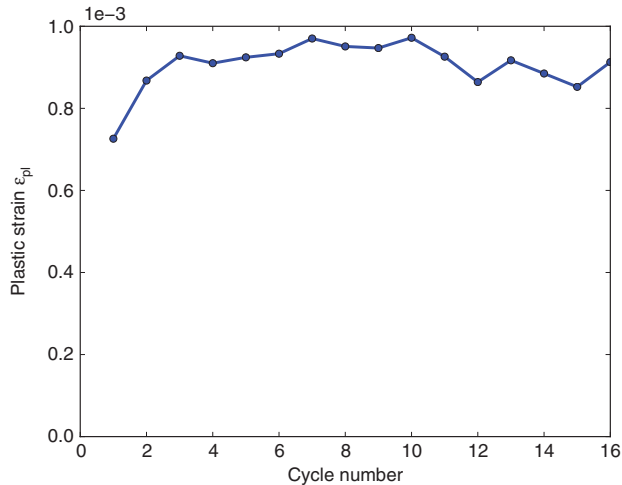


Figure 7: Plastic strain versus number of cycles.

Gertsman et al., 1994; Huang & Ho, 2000). The typical loading rate of fatigue tests is less than 1 s^{-1} .

In the following, a Hall-Petch analysis and Zener-Hollomon analysis will be performed to show how grain size and strain rate effects on stress can be compensated.

Gertsman et al. (1994) have investigated yield stress dependence of copper over a large range of grain sizes. They found that the Hall-Petch relation is best fit by

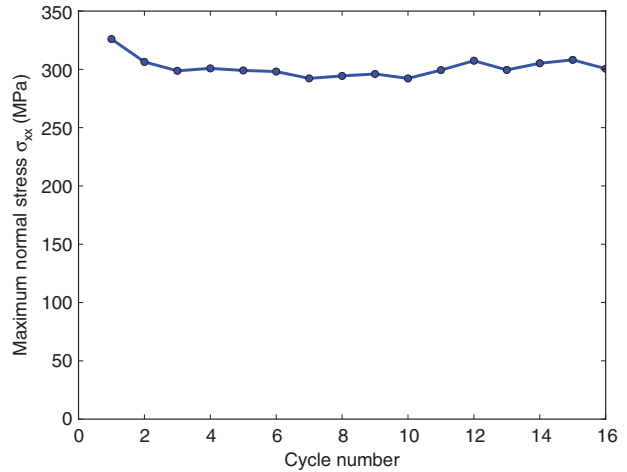


Figure 8: Maximum normal stress versus number of cycles.

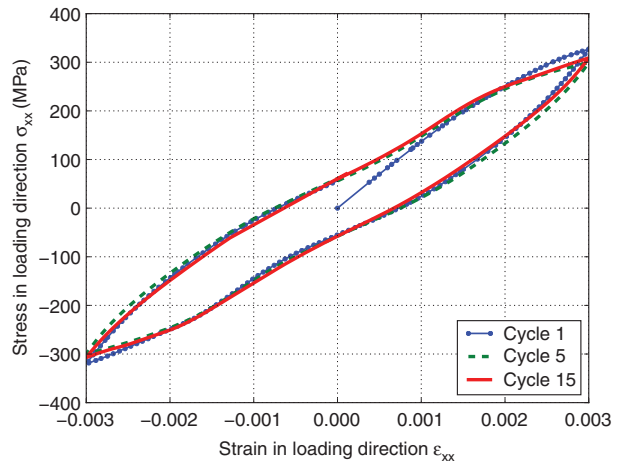


Figure 9: Cyclic stress strain curve.

$$\sigma_y = 92(\pm 12) + 399(\pm 61)d^{-1/2}, \quad (6)$$

where σ_y is the yield stress in MPa and d is the grain size in micrometer. For the grain size of $5 \mu\text{m}$ used in the DD simulations, the yield stress is calculated as $\sigma_y = 270 \text{ MPa}$.

Additionally, the stress-strain curve needs to be adjusted for strain rate. It is known that increase in strain rate has a similar effect as decrease in temperature. As the strain rates shown in the paper are very high (10^5 s^{-1}), this would be equivalent to loading at cryogenic temperatures. Li et al. (2009) investigated the influence of the Zener-Hollomon parameter on the mechanical properties of copper. The Zener-Hollomon parameter Z is given as

$$Z = \dot{\epsilon} \exp\left(\frac{Q}{RT}\right), \quad (7)$$

where T is temperature, R is the gas constant (8.314 J/K/mol), and Q is the activation energy [72.5 kJ/mol for copper (Li et al., 2009)]. An experiment under monotonic quasi-static conditions at room temperature ($\dot{\epsilon} = 10^{-3} \text{ s}^{-1}$, $T = 293 \text{ K}$) has a Z value of 22.0. The Z value for the calculations given in this paper ($\dot{\epsilon} = 10^5 \text{ s}^{-1}$, $T = 293 \text{ K}$) is 41.3. Scaling this value back to quasi-static loading conditions implies a loading temperature of 180 K. It can be seen in the study by Li et al. (2009) that an increase in $\ln(Z)$ from 22 to 41 of a sample strained to 1% will subsequently increase the measured yield stress by approximately 60 MPa. Equivalently, Kwon et al. (1989) showed that the cyclic stress at 0.1% strain increased by 50 MPa from 115 MPa to 165 MPa when going from 298 K to 77 K loading temperature.

Combining the results from Hall-Petch analysis and Zener-Hollomon parameter, the yield stress is in reasonable agreement with experimental results.

Dislocations have a tendency to cluster as depicted in Figure 5, showing the evolution of the dislocation morphology.

At maximum applied tensile and compressive strain, dislocations pile up against the (spherical) grain boundary. During further cycling, more dislocations pile up against the grain boundary. The dislocation pile-up can also be inferred from Figure 10A. The graph shows the number of dislocations contained within a sphere of a given diameter. Between the sphere having the same size as the grain and that only having 95% of the diameter of the grain (20,000 b versus 19,000 b), there is a noticeable jump in dislocation length. This jump represents the dislocations piled up against the grain boundary.

Pile up stress acting on the grain boundary may be mitigated by cross-slip activity and lead to the formation of specific dislocation structures and slip bands during cyclic loading. This mechanism is described in detail by Déprés et al. (2004).

Figure 11 shows the overall evolution of energy. The three largest contributions are losses due to damping E_{damp} , internally stored elastic continuum energy $E_{\text{el,int,cont}}$, and the externally applied work W_{ext} . The continuously rising value of E_{damp} indicates that most work is dissipated as heat and only small amount of work is used to permanently deform the crystal by adding and moving dislocations (E_{core} , E_{self} , and $E_{\text{disl-disl}}$). The increase in dislocation self-energy and core energy is proportional to the increase in dislocation density shown in Figure 6. These energy contributions are independent of other dislocations. The energy due to dislocation-dislocation interaction appears stagnant after a few cycles. This could be explained by the fact that as more dislocations are added to an already

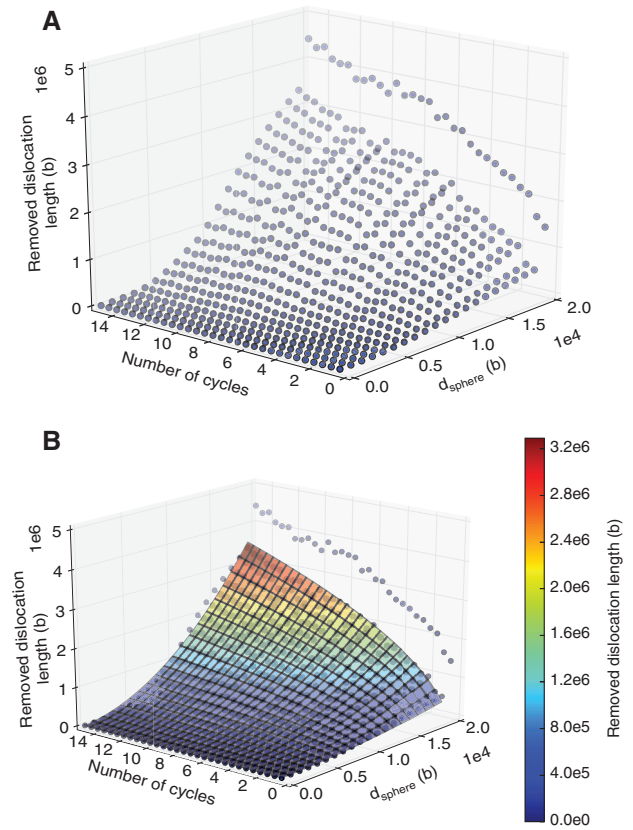


Figure 10: Evolution of dislocation networks. (A) Dislocations lying within volume where crack initiates. (B) Curve fit of dislocations lying within volume where crack initiates.

dense dislocation structure, far field effects are shielded by the already existing dislocation structure and thus only causing local increase in energy.

The sum of all energies is not exactly constant and drifts in the course of the simulation. The drift is about 0.3% after over 2 million increments with respect to the largest energy contribution, and it could be attributed to accumulated rounding errors and the fact that all simulations run with a finite tolerance as well as effects of the topology operations that take place. For example, when segments are refined during the bowing of an arch, the additional node is (depending on the refinement procedure) placed on that arch. This makes the time incrementation scheme more stable, but it also increases dislocation length without any motion involved and it changes location of segments without movement that could be damped.

6.3 Prediction of fatigue life

The methodology described in Section 2 will be extended to allow for the prediction of fatigue crack initiation using

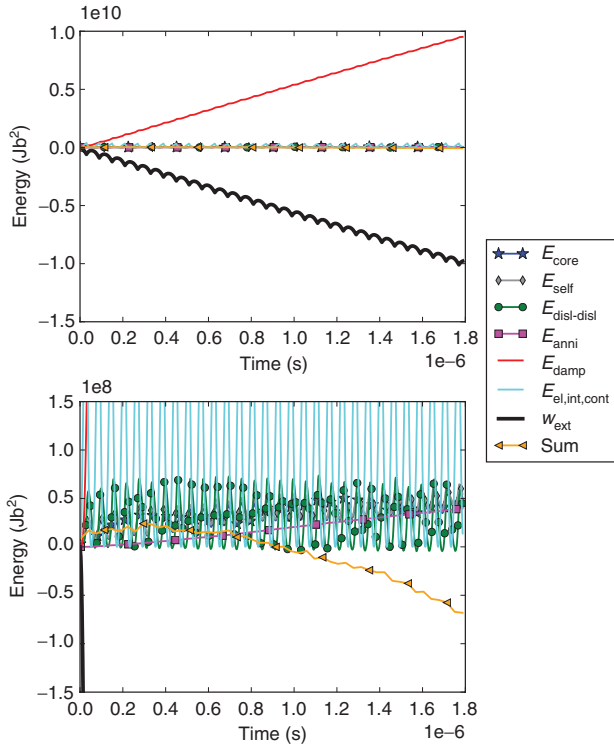


Figure 11: Evolution of energy terms in the DD simulation during fatigue loading. Both curves show the same, with the axes-range of the bottom curve adjusted to better display energy terms of smaller magnitude.

DD simulations. First, an energy balance is created according to equation (1). The dislocation energy is composed of the energy that is stored in the dislocation network and can be recovered once dislocations are removed (for example, by forming a free surface of a crack and getting pushed out). These terms are the self, the core, and the dislocation-dislocation interaction energy,

$$E_{\text{disl}} = E_{\text{core}} + E_{\text{self}} + E_{\text{disl-disl}}. \quad (8)$$

The reduction of elastic energy upon formation of a penny-shaped crack in an infinite medium-loaded normal to the crack plane is given by (Sack, 1946; Sneddon, 1965)

$$E_{\text{cont}} = \frac{8(1-\nu^2)}{3E} \sigma^2 d^3, \quad (9)$$

where E is the elastic modulus, ν is Poisson’s ratio, σ is the applied stress, and d is the diameter of the crack. Finally, the surface energy is given by

$$E_{\text{surf}} = 2A\gamma, \quad (10)$$

where $A = d^2\pi/4$ is the cross-sectional area of the crack, γ is the surface energy per unit area, and factor 2 indicates that two surfaces were formed. The surface energy of pure copper is taken to be 1725 mJ/m² (McLean, 1957).

Once a crack is formed, the size of the crack should be related to the number of dislocations involved in forming the crack. Mura and Nakasone (1990) used an extrusion model in 2D that related the crack size c to the number of dislocations N and Burgers vector magnitude b as $c = Nb$. This is generalized here for three dimensions $A = bl$, where l is the length of dislocations involved in forming the crack and b is the Burgers vector magnitude.

Not all dislocations present in the simulation are used to form a crack. Dislocations need to be close to each other. In the determination of the size of the hypothetical crack, the following assumption will be made: the cross-section of a penny-shaped crack is equal to the Burgers vector times the length of dislocations contained in a sphere of the same diameter.

$$bl = \frac{\pi}{4} d^2 \quad (11)$$

This statement is also illustrated in Figure 12. The dislocation band in a given volume is removed, and a crack of the same size is created instead. This assumption is motivated by the computational complexity of the problem. More precise calculations could be performed by considering different volume types other than a sphere (for example, a cylinder of certain height), and those volumes can be placed at arbitrary locations and orientations within the simulation box, which try to maximize the energy within that volume.

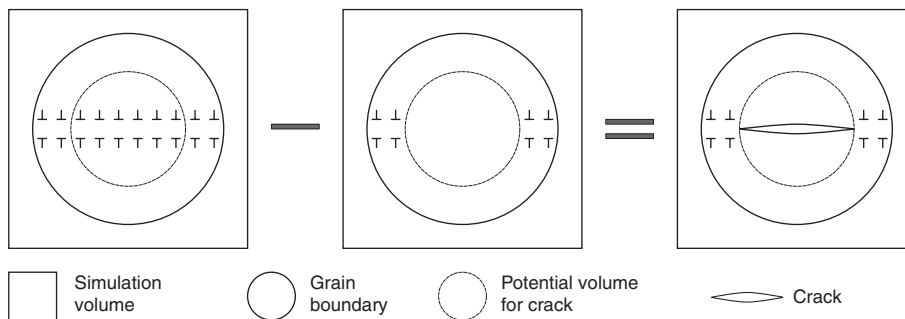


Figure 12: Volume where dislocations are removed to create a crack.

Due to the computational intensive nature of DD simulations, it is currently only possible to run tens of cycles in a reasonable amount of time (the simulations presented in this section take about 4 weeks using 128 CPUs). On the other hand, for the strain levels presented, fatigue crack initiation and failure occur after hundreds to thousands of cycles. Therefore, the results of the DD simulations will be extrapolated in time and space.

First, the evolution of dislocation length will be investigated. Figure 10A and B show the length of dislocations that might be removed to form a crack as a function of volume size considered and number of cycles. It can be noted that between a diameter of 20,000 b (the grain diameter) and 19,000 b, a large jump occurs, which is due to dislocations piling up against the grain boundary.

The interpolation chosen for length of dislocations that can be used to form a crack is composed of a part describing the evolution in time and one describing the evolution in space. The evolution in space is a Taylor expansion up to second order, where the constant term is zero, because a sphere of zero diameter should not contain any dislocations. The evolution with respect to number of cycles follows a power law, similar to what has been observed by Huang et al. (2008) and used by Sangid et al. (2011). Especially, the increase in dislocation density versus number of cycles is chosen as a square root, which is slower than predicted by Mura and Nakasone (1990) and Fine and Bhat (2007) (linear) and faster than what is predicted by Brinckmann (2005) (logarithmic).

The resulting equation has the form

$$l = (C_{11}d + C_{12}d^2)(\sqrt{n} + C_{13}). \quad (12)$$

The curve fit of this equation is shown in Figure 13B. Equation (12) needs to be combined with equation (11) to give a relation between the potential crack size and number of cycles. Combining these equations leads to

$$d = \frac{C_{11}(\sqrt{n} + C_{13})}{\pi/(4b) - C_{12}(\sqrt{n} + C_{13})}. \quad (13)$$

The interpolation chosen for the energy stored in the dislocations that are removed upon initiation of a crack is

$$E_{\text{disl}} = C_{d1}d^2(\sqrt{n} + C_{d2}). \quad (14)$$

The interpolation values are given in Table 3, with all values referring to SI units.

Equation (13) can be inserted into equations (9) and (10), and with equation (14), all terms of the Gibbs free energy of a hypothetical crack are defined. The different terms of equation (1) are plotted individually and as a sum in Figure 14. It can be seen that the Gibbs free energy

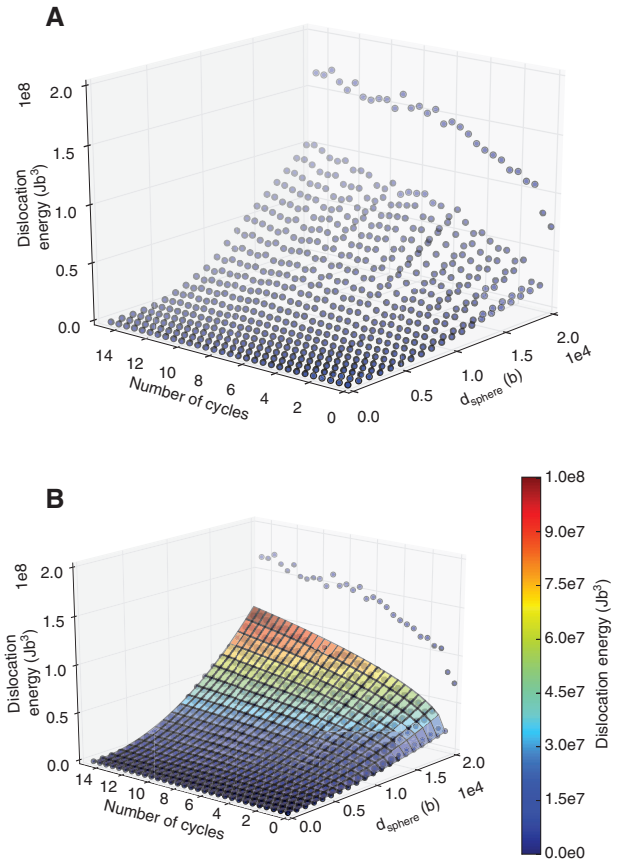


Figure 13: Evolution of dislocation networks. (A) Energy of dislocations in certain volume available for crack initiation. (B) Curve fit of energy of dislocations in certain volume available for crack initiation.

Table 3: Interpolation values for equations (12) and (14).

C_{11}	6.4249
C_{12}	9.3669×10^6
C_{13}	-0.2930
C_{d1}	0.0655
C_{d2}	0.9697

attains a maximum around 840 cycles. At that point, the dislocation structure formed so far becomes unstable, and it would be energetically more favorable to form a real crack. This is the value at which a fatigue crack is initiated. The size of the predicted initiated crack is about 0.13 μm .

7 Comparison with experimental results

The fatigue behavior of oxygen-free high thermal conductivity copper has been studied extensively in the literature.

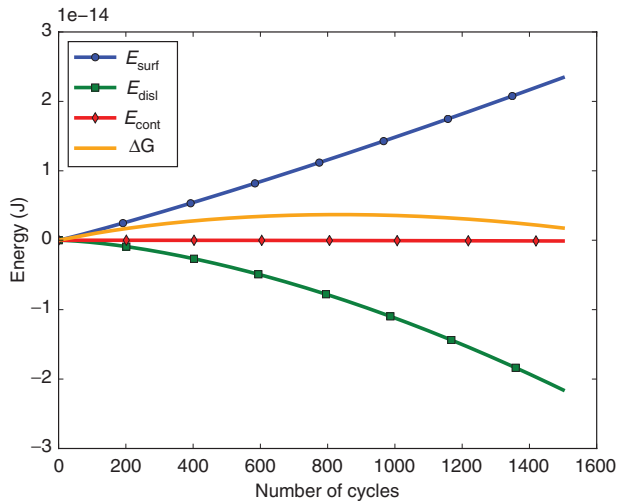


Figure 14: Gibbs free energy of a hypothetical crack nucleating.

However, most information is given either for stress versus (plastic) strain or cycles until full failure. On the other hand, data for number of cycles until fatigue crack initiation are much more scarce probably due to the difficulty in observing fatigue crack initiation. Therefore, data are reported for both fatigue crack initiation and fatigue failure in this section. Results for fatigue crack initiation and fatigue life are given in Figure 15. The following comments are important with respect to that figure:

- Kwon et al. (1989) have investigated the initiation and growth of small fatigue cracks at 298, 77, and 4.2 K in polycrystalline copper. They state that their definition of fatigue crack is chosen quite arbitrarily and related to the resolution of the observation technique. They defined “just initiated” as an impression of 100 μm .

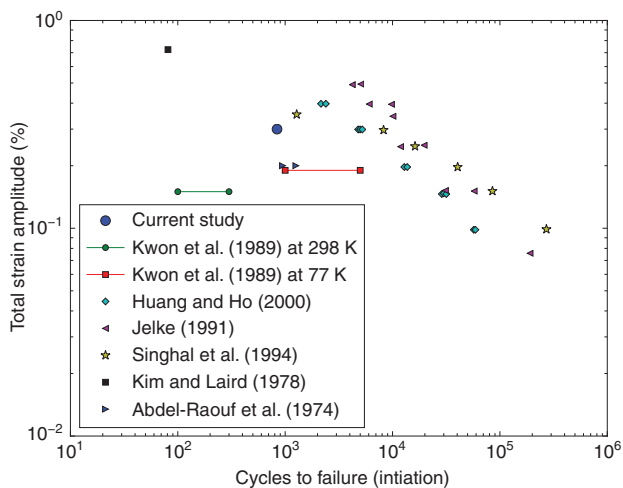


Figure 15: Experimental results of fatigue crack initiation and fatigue life of OFHC copper compared to current study.

With this definition, a specimen cycled at room temperature at $\Delta\varepsilon/2 = 1.5 \times 10^{-3}$ shows fatigue crack initiation between 100 and 300 cycles. A specimen cycled at liquid nitrogen temperature (77 K) and $\Delta\varepsilon/2 = 1.9 \times 10^{-3}$ shows fatigue crack initiation between 1000 and 5000 cycles.

- Kim and Laird (1978) have investigated crack initiation in high strain fatigue. After straining a specimen at a plastic strain amplitude of $\Delta\varepsilon_{pl} = 0.57\%$ for 81 cycles, they observed indication for a crack nucleus along the grain boundary. The data point is added to Figure 15 assuming a plateau stress of $\sigma_{max} = 180$ MPa (Eckert et al., 1987) and a macroscopic elastic modulus of $E = 117$ GPa as $\Delta\varepsilon/2 = \Delta\varepsilon_{pl}/2 + \sigma_{max}/E$.
- Huang and Ho (2000) studied the emergence of fatigue cracks. Experiments were strain controlled and stopped when fatigue cracks were visible under the microscope.
- Jelke (1991) investigated low cycle fatigue crack initiation and propagation in OFHC copper. The experiments were strain controlled but only with an R-value of 0. The reported values are fatigue life values.
- Singhal et al. (1994) reported cycles to failure for OFHC copper at a total strain controlled experiment.
- Abdel-Raouf et al. (1974) investigated OFHC copper at various strain ranges and temperatures. The data in Figure 15 are at room temperature, and strain rates of $\dot{\varepsilon} = 4 \times 10^{-1} \text{ s}^{-1}$ and $\dot{\varepsilon} = 4 \times 10^{-3} \text{ s}^{-1}$. Slower loading rates reduce number of cycles to failure compared to faster loading rates, but this effect was found to be much more significant at elevated temperatures. The reported values are cycles to failure.

Compared to experimental results available in the literature, the results of the current study show fatigue crack initiation at reasonable but somewhat lower values. This might be due to the following: (1) The values reported by Jelke (1991) and Singhal et al. (1994) are cycles to full fatigue failure after crack propagation and therefore expected to be significantly above the value for fatigue crack initiation. The values are included to give an upper bound. (2) Huang and Ho (2000) reported values for fatigue crack initiation, but the question always remains, at what point in time an initiated fatigue crack is detectable experimentally under the microscope. Typically, crack nucleation at the surface is detectable due to emergence of dislocation and slip lines. (3) The proposed DD and energy-based theory uses all of the energy stored in the dislocation networks within a certain volume. In reality, only a part of the dislocations are pushed out to form a free surface and some dislocations might be remaining.

Therefore, only part of the energy stored in the dislocation network is used, and accordingly, more cycles would be necessary to initiate a fatigue crack.

7.1 Influence of environmental conditions

The proposed method for fatigue crack initiation can be extended to account for environmental effects by adjusting the surface energy γ_s . The surface energy can be reduced by the adsorption of foreign atoms. For example, in steels with phosphorous, tin, or antimony and aluminum with gallium or mercury, embrittlement can be observed from the introduction of foreign atoms and reduction in cohesive energy (Vasudevan, 2013). The influence of impurities in copper has been experimentally studied at grain boundaries. There is indication that segregation of less than one monolayer of Bi atoms can lead to significant changes in the electronic structure, resulting in a large drop in the work of fracture in Cu bicrystals. Recently, the embrittlement of aluminum alloy Al 7075 by liquid metal (Ga) was investigated. An increase in Ga atoms leads to a drastic decrease in surface energy and plastic work (Ganesan & Sundararaghavan, 2015).

The reduction in surface energy that is needed to form a free surface can now be reliably calculated for a variety of atomic arrangements using density functional theory (Dawson et al., 1996).

Figure 16 shows the influence of surface energy on number of cycles to failure for copper fatigued at 0.3% strain amplitude. As expected, a decrease in surface energy causes a decrease in number of cycles to failure.

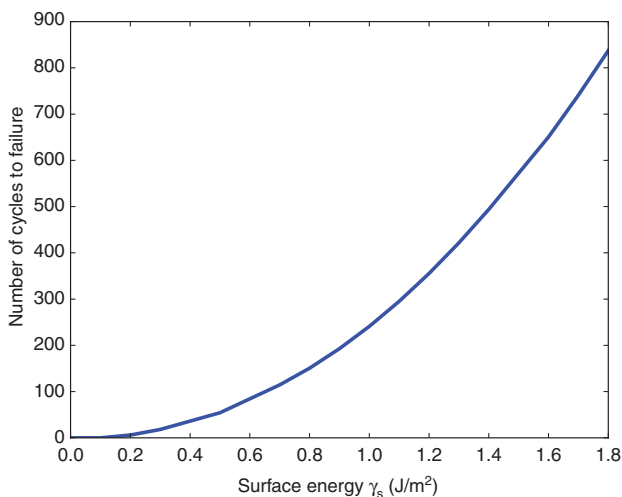


Figure 16: Influence of surface energy γ_s on number of cycles until failure.

7.2 Limitations of the proposed method

The model proposed in this paper is aiming to predict fatigue crack initiation based on the energy stored in the system. This approach follows the spirit of Mura (1994), Mura and Nakasone (1990), Bhat & Fine (2001), Fine & Bhat (2007), and others (Li et al., 2015; Naderi et al., 2016). The difference to previous approaches is that DD simulations are used directly to construct the energy balance as opposed to analytical expression or CPFE.

As such, the current approach aims to use less approximations than those in the cited papers. On the other hand, it does not take into account specific micro-structural configurations. The current criterion is only concerned with the energy that could be utilized by removing dislocations in a given volume. As the proposed criterion does not distinguish micro-structures beyond this point, no statements can be or are attempted to be made about the specific local microstructural mechanisms that rule the initiation of the crack and whether the initiated cracks are, for example, shear cracks, grain boundary cracks, or others.

The current approach only considers fatigue crack initiation, not propagation. Once initiation is detected, progression would need to be handled in an engineering fashion, for example, by using Paris' law.

Furthermore, the presented methodology assumes that the evolution of dislocation density follows a specific trend that can be extrapolated from a limited number of calculated cycles. Based on other theoretical (Sangid et al., 2011) and experimental (Huang et al., 2008) works, a power law is used for extrapolation. However, due to the large computational requirements of DD simulations, it is currently not possible to verify this assumption.

The extrapolation scheme used in this paper assumes that dislocation density continues to increase, however, with decreasing rate. On the other hand, dislocation density of copper cycled at room temperature in the LCF regime generally saturates before fatigue crack initiation can be detected. For the theory presented in this paper to yield meaningful results, at least the energy stored in the dislocation network needs to increase. This could be achieved, for example, by changing the relative arrangement of the dislocations at constant dislocation density. If such behavior were the case, compared to an increase in both dislocation density and energy as presented in this paper, the crack initiation would be shifted to a lower cycle number, as more energy is available to create a crack of constant size.

It should be kept in mind that the computational requirements of DD necessitate a high strain rate, which

is qualitatively equivalent to quasi-static loading at low temperatures via a Zener-Holloman relationship.

Polák (1987) investigated fatigue in copper at liquid helium temperature and plastic strain amplitude of 2.5×10^{-3} . It appears that in the range investigated, up to 2000 cycles dislocation production rates are positive.

Also, Kwon et al. have shown that hardening curves for a strain amplitude of $\Delta\varepsilon/2=0.15\%$ start to saturate at room temperature starting at 100 cycles and being fully saturated at 1000 cycles. In that case, they report a fatigue crack initiation between 100 and 300 cycles. For liquid nitrogen at a strain amplitude $\Delta\varepsilon/2=0.19\%$, saturation is not finished until 10^4 cycles. The reported fatigue crack initiation range is between 1000 and 5000. The loading conditions presented in this paper with respect to temperature and loading rate fall in a similar range.

8 Conclusion

A theoretical approach is proposed to predict fatigue crack initiation using DD and an energy-based criterion. The theoretical approach is based on an energy balance of the surface energy and continuum energy loss of a hypothetical crack and the energy stored in the dislocation networks that grow as cycling progresses. Once it is energetically more favorable to form a free surface and push out dislocations than continued dislocation accumulation, a crack was formed. All relevant energies in DD simulations were identified and shown to be consistent, with a small drift in the sum of all energies due to numerically accumulated errors over a large number of simulation increments. The methodology was applied to fatigue crack initiation in an OFHC copper grain of 5- μm diameter, cyclically loaded with 0.3% total strain amplitude. An increase in dislocation density and the energy stored in the dislocation networks is observed. Due to the computational intensive nature of DD simulations, the results were extrapolated from 15 cycles to thousands of cycles. The energy balance or Gibbs free energy of the hypothetical crack showed a maximum and, as a result, initiation of a fatigue crack at 840 cycles. This is in reasonable agreement with experimental data. Finally, it is shown how a decrease in surface energy due to introduction of foreign atoms decreases the number of cycles to failure.

As the capabilities of high-performance computing increase and as DD computer codes are further refined, DD may become a helpful way to estimate LCF initiation lifetimes based on dislocation accumulation.

While this is the first work where a path towards identifying crack initiation using cyclic DD is proposed, several

other parametric studies will be beneficial as and when better computational infrastructures become available. This includes studying the effect of grain size, polycrystals effects, lower strain rates, higher maximum strain, and improved mobility values, and the effect of numerical properties such as segment length, initial imperfections, time integration schemes, and integration tolerance may also be tested.

Acknowledgments: This work was supported by the U.S. Department of Energy, Office of Basic Energy Sciences, Division of Materials Sciences and Engineering under Award #DE-SC0008637 as part of the Center for Predictive Integrated Structural Materials Science (PRISMS Center) at the University of Michigan.

References

- Abdel-Raouf H, Plumtree A, Topper TH. Temperature and strain rate dependence of cyclic deformation response and damage accumulation in OFHC copper and 304 stainless steel. *Metall Trans* 1974; 5: 267–277.
- Amodeo RJ, Ghoniem NM. Dislocation dynamics. II. Applications to the formation of persistent slip bands, planar arrays, and dislocation cells. *Phys Rev B* 1990; 41: 6968–6976.
- Antonopoulos JG, Brown LM, Winter AT. Vacancy dipoles in fatigued copper. *Philos Mag* 1976; 34: 549–563.
- Arsenlis A, Cai W, Tang M, Rhee M, Opperstrup T, Hommes G, Pierce TG, Bulatov VV. Enabling strain hardening simulations with dislocation dynamics. *Modell Simul Mater Sci Eng* 2007; 15: 553–595.
- Arsenlis A, Aubry S, Bulatov V, Cai W, Hommes G, Opperstrup T, Pierce T, Rhee T, Tang M. *ParaDiS User's Guide – Version 2.5.1 – public*. Lawrence Livermore National Laboratory, 2011.
- Basinski ZS, Basinski SJ. Fundamental aspects of low amplitude cyclic deformation in face-centred cubic crystals. *Prog Mater Sci* 1992; 36: 89–148.
- Benzerga AA, Bréchet Y, Needleman A, Van der Giessen E. Incorporating three-dimensional mechanisms into two-dimensional dislocation dynamics. *Modell Simul Mater Sci Eng* 2004; 12: 159–196.
- Bhat SP, Fine ME. Fatigue crack nucleation in iron and a high strength low alloy steel. *Mater Sci Eng A* 2001; 314: 90–96.
- Brinckmann S. On the role of dislocation in fatigue crack initiation, PhD thesis, University of Groningen, 2005.
- Bulatov V, Cai W. *Computer simulation of dislocations*. Oxford: Oxford University Press, 2006.
- Bulatov V, Cai W, Fier J, Hiratani M, Hommes G, Pierce T, Tang M, Rhee M, Yates K, Arsenlis T. Scalable line dynamics in paradis. In: *Proceedings of the ACM/IEEE Super Computing 2004 Conference*, Pittsburgh, 2004.
- Cai W, Arsenlis A, Weinberger CR, Bulatov V. A non-singular continuum theory of dislocations. *J Mech Phys Solids* 2006; 54: 561–587.

- Dawson I, Bristowe PD, Lee MH, Payne MC, Segall MD, White JA. First-principles study of a tilt grain boundary in rutile. *Phys Rev B* 1996; 54: 13727–13733.
- Déprés C, Robertson CF, Fivel MC. Low-strain fatigue in AISI 316L steel surface grains: a three-dimensional discrete dislocation dynamics modelling of the early cycles I. Dislocation microstructures and mechanical behaviour. *Philos Mag* 2004; 84: 2257–2275.
- Déprés C, Reddy GVP, Robertson C, Fivel M. An extensive 3D dislocation dynamics investigation of stage-I fatigue crack propagation. *Philos Mag* 2014; 94: 4115–4137.
- Deshpande VS, Needleman A, Van der Giessen E. Discrete dislocation plasticity modeling of short cracks in single crystals. *Acta Mater* 2003; 51: 1–15.
- Eckert R, Laird C, Bassani J. Mechanism of fracture produced by fatigue cycling with a positive mean stress in copper. *Mater Sci Eng* 1987; 91: 81–88.
- Escaig B. Sur le glissement dévié des dislocations dans la structure cubique à faces centrées. *Journal des Physique* 1968; 29: 225–239.
- Essmann U, Mughrabi H. Annihilation of dislocations during tensile and cyclic deformation and limits of dislocation densities. *Philos Mag A* 1979; 40: 731–756.
- Essmann U, Gösele UG, Mughrabi H. A model of extrusions and intrusions in fatigued metals I. Point-defect production and the growth of extrusions. *Philos Mag A* 1981; 44: 405–426.
- Fine ME, Bhat SP. A model of fatigue crack nucleation in single crystal iron and copper. *Mater Sci Eng A* 2007; 468–470: 64–69.
- Finney JM, Laird C. Strain localization in cyclic deformation of copper single crystals. *Philos Mag* 1975; 31: 339–366.
- Fleischer RL. Cross slip of extended dislocations. *Acta Metall* 1959; 7: 134–135.
- Forsyth PJE. Exudation of material from slip bands at the surface of fatigued crystals of an aluminium-copper alloy. *Nature* 1953; 171: 172–173.
- Ganesan S, Sundararaghavan V. An atomistically-informed energy based theory of environmentally assisted failure. *Corros Rev* 2015; 33: 455–465.
- Gardner DJ, Woodward CS, Reynolds DR, Hommes G, Aubry S, Arsenlis A. Implicit integration methods for dislocation dynamics. *Modell Simul Mater Sci Eng* 2015; 23: 1–31.
- Gertsman VY, Hoffmann M, Gleiter H, Birringer R. The study of grain size dependence of yield stress of copper for a wide grain size range. *Acta Metall Mater* 1994; 42: 3539–3544.
- Henager Jr CH., Hoagland RG. Dislocation and stacking fault core fields in FCC metals. *Philos Mag* 2005; 85: 4477–4508.
- Huang HL, Ho NJ. The study of fatigue in polycrystalline copper under various strain amplitude at stage I: crack initiation and propagation. *Mater Sci Eng A* 2000; 293: 7–14.
- Huang E-W, Barabash RI, Wang Y, Clausen B, Li L, Liaw PK, Ice GE, Ren Y, Choo H, Pike LM, Klarstrom DL. Plastic behavior of a nickel-based alloy under monotonic-tension and low-cycle-fatigue loading. *Int J Plast* 2008; 24: 1440–1456.
- Huang M, Tong J, Li Z. A study of fatigue crack tip characteristics using discrete dislocation dynamics. *Int J Plast* 2014; 54: 229–246.
- Jelke BE. Low cycle fatigue and crack growth in oxygen free high conductivity copper, Masters thesis, University of Illinois at Urbana-Champaign, 1991.
- Joseph DS, Chakraborty P, Ghosh S. Wavelet transformation based multi-time scaling method for crystal plasticity FE simulations under cyclic loading. *Comput Method Appl Mech Eng* 2010; 199: 2177–2194.
- Kim WH, Laird C. Crack nucleation and stage I propagation in high strain fatigue-I. Microscopic and interferometric observations. *Acta Metall* 1978; 26: 777–787.
- Kwadjo R, Brown LM. Cyclic hardening of magnesium single crystals. *Acta Metall* 1978; 26: 1117–1132.
- Kwon IB, Fine ME, Weertman J. Fatigue damage in copper single crystals at room and cryogenic temperatures. *Acta Metall* 1989; 37: 2937–2946.
- Li YS, Zhang Y, Tao NR, Lu K. Effect of the zener-hollomon parameter on the microstructures and mechanical properties of Cu subjected to plastic deformation. *Acta Mater* 2009; 57: 761–772.
- Li L, Shen L, Proust G. Fatigue crack initiation life prediction for aluminium alloy 7075 using crystal plasticity finite element simulations. *Mech Mater* 2015; 81: 84–93.
- Lukáš P, Klesnil M, Krejčí J. Dislocations and persistent slip bands in copper single crystals fatigued at low stress amplitude. *Phys Status Solidi B* 1968; 27: 545–558.
- McLean D. Grain boundaries in metals. Oxford: Clarendon Press, 1957.
- Mott NF. A theory of the origin of fatigue cracks. *Acta Metall* 1958; 6: 195–197.
- Mughrabi H. The cyclic hardening and saturation behaviour of copper single crystals. *Mater Sci Eng* 1978; 33: 207–223.
- Mughrabi H, Wang R. Cyclic strain localization and fatigue crack initiation in persistent slip bands in face-centred cubic metals and single-phase alloys. In: Sih GC, Zorski H, editors. *Defects and fracture*. Netherlands: Springer, 1982: 15–28.
- Mura T. A theory of fatigue crack initiation. *Mater Sci Eng A* 1994; 176: 61–70.
- Mura T, Nakasone Y. A theory of fatigue crack initiation in solids. *J Appl Mech* 1990; 57: 1–6.
- Naderi M, Amiri M, Iyyer N, Kang P, Phan N. Prediction of fatigue crack nucleation life in polycrystalline AA7075-T651 using energy approach. *Fatigue Fract Eng Mater Struct* 2016; 39: 167–179.
- Orowan E. Energy of fracture. *Weld J. Res Supplement* 1955; 20: 157–160.
- Polák J. Resistivity of fatigued copper single crystals. *Mater Sci Eng* 1987; 89: 35–43.
- Sack RA. Extension of Griffith's theory of rupture to three dimensions. *Proc Phys Soc* 1946; 58: 729.
- Sanford RJ. Principles of fracture mechanics. Upper Saddle River, NJ: Pearson Education, Inc., 2002.
- Sangid MD. The physics of fatigue crack initiation. *Int J Fatigue* 2013; 57: 58–72.
- Sangid MD, Maier HJ, Sehitoglu H. A physically based fatigue model for prediction of crack initiation from persistent slip bands in polycrystals. *Acta Mater* 2011; 59: 328–341.
- Shin CS, Robertson CF, Fivel MC. Fatigue in precipitation hardened materials: a three-dimensional discrete dislocation dynamics modelling of the early cycles. *Philos Mag* 2007; 87: 3657–3669.
- Singhal A, Stubbins JF, Singh BN, Garner FA. Fusion reactor materials room temperature fatigue behavior of OFHC copper and CuAl25 specimens of two sizes. *J Nucl Mater* 1994; 212: 1307–1312.

- Sneddon IN. A note on the problem of the penny-shaped crack. *Math Proc Cambridge Philos Soc* 1965; 61: 609–611.
- Stevenson R, Vander Sande JB. The cyclic deformation of magnesium single crystals. *Acta Metall* 1974; 22: 1079–1086.
- Tanaka K, Mura T. A dislocation model for fatigue crack initiation. *J Appl Mech* 1981; 48: 97–103.
- Vasudevan AK. Applied stress affecting the environmentally assisted cracking. *Metall Mater Trans A* 2013; 44: 1254–1267.
- Venkataraman G, Chung YW, Mura T. Application of minimum energy formalism in a multiple slip band model for fatigue – I. Calculation of slip band spacings. *Acta Metall Mater* 1991; 39: 2621–2629.
- Winter AT. A model for the fatigue of copper at low plastic strain amplitudes. *Philos Mag* 1974; 30: 719–738.
- Yumen L, Huijiu Z. Dislocation structures in a ferrite steel. *Mater Sci Eng* 1986; 81: 451–455.
- Zbib HM. Introduction to discrete dislocation dynamics. In: Carlo S, Sebastian S, editors. *Generalized continua and dislocation theory*, Volume 537 of CISM Courses and Lectures. Vienna: Springer, 2012: 289–317.
- Zhang ZF, Gu HC, Tan XL. Low-cycle fatigue behaviors of commercial-purity titanium. *Mater Sci Eng A* 1998; 252: 85–92.